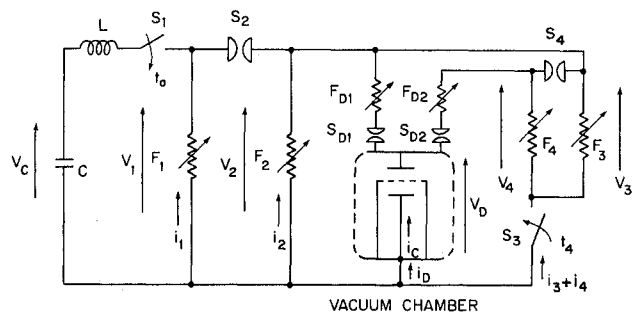


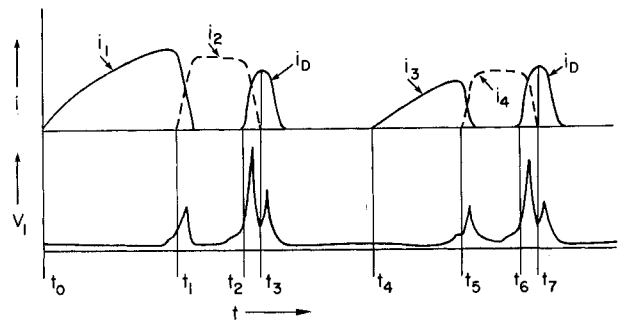
Naval Research Laboratory
Washington, DC 20375

II. Experimental Configuration

A schematic of the inductive storage system used to provide two pulses across an electron beam diode is shown in Figure 1. Wire fuses in air were used as opening switches. Each pulse was generated by two fuse stages, the second stage producing the high voltage associated with each pulse. For single pulse operation, the wire fuses F_{D2} , F_4 and F_3 were removed from the system. Switch S_3 is an explosively driven switch which holds off the entire voltage associated with the first pulse and closes with relatively little voltage across it.



All the other closing switches are spark gaps set to self-break at the appropriate voltage, except for switch S_1 , which is command triggered to initiate the firing sequence. A graphical depiction of the voltage and current waveforms is given in Figure 2. Note that t_3 and t_7 correspond to the times when fuses F_{D1} and F_{D2} , respectively, are opened.



One major problem associated with the use of inductive storage systems for repetitive electron beam production that has not been studied sufficiently is the diode recovery between pulses*. Plasma formed during¹⁰ and after beam generation may affect the diode characteristics for subsequent pulses in repetitive systems. These effects are particularly important to inductive systems because of their characteristically long L/R decay time and slow (compared to capacitive systems) risetime. The plasma production in the diode and its recovery characteristics are also related to the processes occurring in vacuum current interrupters, including those being developed for repetitive switching.¹¹

The storage system (Fig. 1, $C=240\text{ }\mu\text{F}$, $L=7\text{ }\mu\text{H}$, $V_C \approx 9\text{ kV}$) is similar to that used in the study of recovery characteristics of fuses used as opening switches.¹² Sufficient energy is stored at low voltage in the capacitor so that the requirements, (e.g., energy dissipated in opening the fuses) for generating two pulses are satisfied.

*External magnetic fields have been used, e.g., in foilless diodes, to suppress plasma effects.^{8,9}

Report Documentation Page				Form Approved OMB No. 0704-0188	
Public reporting burden for the collection of information is estimated to average 1 hour per response, including the time for reviewing instructions, searching existing data sources, gathering and maintaining the data needed, and completing and reviewing the collection of information. Send comments regarding this burden estimate or any other aspect of this collection of information, including suggestions for reducing this burden, to Washington Headquarters Services, Directorate for Information Operations and Reports, 1215 Jefferson Davis Highway, Suite 1204, Arlington VA 22202-4302. Respondents should be aware that notwithstanding any other provision of law, no person shall be subject to a penalty for failing to comply with a collection of information if it does not display a currently valid OMB control number.					
1. REPORT DATE JUN 1981		2. REPORT TYPE N/A		3. DATES COVERED -	
4. TITLE AND SUBTITLE Inductive Pulsed-Power System For Repetitive Operation Of Electron-Beam Diodes				5a. CONTRACT NUMBER	
				5b. GRANT NUMBER	
				5c. PROGRAM ELEMENT NUMBER	
6. AUTHOR(S)				5d. PROJECT NUMBER	
				5e. TASK NUMBER	
				5f. WORK UNIT NUMBER	
7. PERFORMING ORGANIZATION NAME(S) AND ADDRESS(ES) Naval Research Laboratory Washington, DC 20375				8. PERFORMING ORGANIZATION REPORT NUMBER	
9. SPONSORING/MONITORING AGENCY NAME(S) AND ADDRESS(ES)				10. SPONSOR/MONITOR'S ACRONYM(S)	
				11. SPONSOR/MONITOR'S REPORT NUMBER(S)	
12. DISTRIBUTION/AVAILABILITY STATEMENT Approved for public release, distribution unlimited					
13. SUPPLEMENTARY NOTES See also ADM002371. 2013 IEEE Pulsed Power Conference, Digest of Technical Papers 1976-2013, and Abstracts of the 2013 IEEE International Conference on Plasma Science. Held in San Francisco, CA on 16-21 June 2013. U.S. Government or Federal Purpose Rights License.					
14. ABSTRACT					
15. SUBJECT TERMS					
16. SECURITY CLASSIFICATION OF:			17. LIMITATION OF ABSTRACT SAR	18. NUMBER OF PAGES 4	19a. NAME OF RESPONSIBLE PERSON
a. REPORT unclassified	b. ABSTRACT unclassified	c. THIS PAGE unclassified			

beam to reach a collector plate located behind the anode-cathode gap and to prevent plasma from reaching the collector. For these experiments the cathode consisted of sawblades and the anode shield opening diameter was 10 cm.

Diagnostics consisted of a voltage divider to measure the diode voltage, V_D ; calibrated Rogowski loops to measure the diode current, i_D , and collector current, i_C (Fig. 1); a streak camera to observe the light emitted by the diode plasma; and a photomultiplier with collimation optics to provide spatial resolution along a line of sight perpendicular to the axis of the diode.

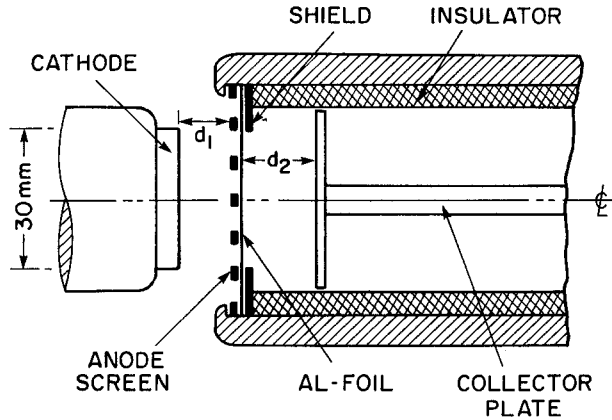


Figure 3. Schematic of the electrode and collector structure of the two-pulse diode.

III. Single Pulse Operation

A. Beam Generation

The current and voltage across the diode for a cathode area of 7 cm^2 and an anode-cathode gap of 1.5 cm as well as the electron beam current into the collector and the diode impedance are shown in Figure 4. The inductive component of the diode voltage was $\leq 5\%$ of the signal and was therefore neglected. The voltage pulse risetime, consisting of two different components, is determined by the characteristics of the switch (S_2) closing and fuse (F_2) opening. The diode current of about 1 kA, consists initially of the electron beam (part of which is also intercepted by the collector) and in later phases ($\geq 250 \text{ nsec}$) of the plasma current. This late time current is not directly associated with the beam (as evidenced by i_C decreasing after $\sim 250 \text{ nsec}$) but rather is being carried by the arc plasma¹³ that forms in the anode-cathode gap subsequent to the beam generation. At the anode, the beam area was determined to be $\sim 20 \text{ cm}^2$ from blue cellophane¹⁴ placed behind the aluminum foil giving a mean beam current density at the anode of $\sim 50 \text{ A/cm}^2$. The behavior of the diode impedance, Z , is typical for diodes where whisker plasma expansion is present. The impedance collapse at time $\geq 250 \text{ nsec}$ is a result of the diode plasma providing a short circuit across the diode. The time of onset and rate of collapse are consistent with the parameters reported elsewhere.^{2,10,15}

B. Plasma Formation and Life Time

The plasma in the diode, present after the impedance collapse, has been observed with a streak camera and a collimated photomultiplier, RCA 1P28A. The streak camera, with a slit aligned perpendicular to the diode axis shows the appearance of plasma (with sufficient density to expose the film) at about 500 nsec after voltage application to the diode. This is a

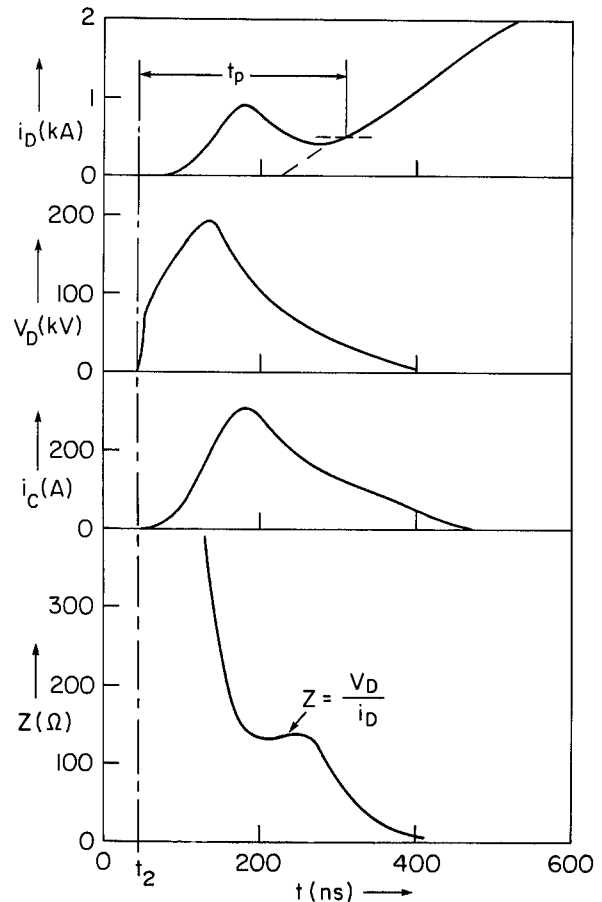


Figure 4. Current, i_D , and voltage, V_D , across the electron beam diode. Also shown are the component of the electron beam measured by the collector plate, i_C , and diode impedance determined from i_D and V_D .

little later than the onset of the current in the diode due to plasma. The light emission recorded on the streak, suggests that the initial whisker plasma is at lower density, insufficient to be recorded on the film. It follows from this that the arc plasma dominates the plasma production when an inductive storage system with post-pulse current is used. To reduce the effects of this current a fuse F_{D1} (shown in the diagram of Fig. 1) is used. The choice of cross section for this fuse determines the time when the diode current can be interrupted. The earlier the interruption, the less plasma is produced. The typical time history of the light emission as observed by the photomultiplier shows that the light persists for some microseconds after the current has ceased. The persistence may be a consequence of the characteristic recombination and plasma expansion times. This point will be discussed further.

IV. Double Pulse Operation

To achieve high voltage second pulse operation the circuit of Fig. 1 was employed. When sufficient energy is stored in the capacitor (relative to that dissipated by fuses and e-beam load of the first pulse) the circuit provides a very convenient method for generating two pulses with a variable (10–500 μs) separation between pulses. The first-pulse fuses and the fuse inserted in the diode branch totally block the discharge of energy until the explosively actuated (high stand-off voltage, low trigger voltage) closing switch, S_3 , is fired. At that time, current through

the second-pulse fuses leads to their vaporization and results in the generation of a second pulse (t_6 , Fig. 2).

The diode characteristics are shown in Fig. 5 (in analogy to Fig. 4 for single pulse operations). Type 1 discharges, indicated by solid lines, show a similar behavior to the single pulse observations. The delay between pulses necessary to obtain the behavior is $\geq 100 \mu\text{sec}$. The early time behavior of the second voltage pulse differs some from that of the first. This may be caused by the diode environment or the details of the second pulse circuitry. In general the beam current and voltage are lower for the second pulse than for the first owing primarily to the fact that much of the stored energy is consumed in producing the first pulse.

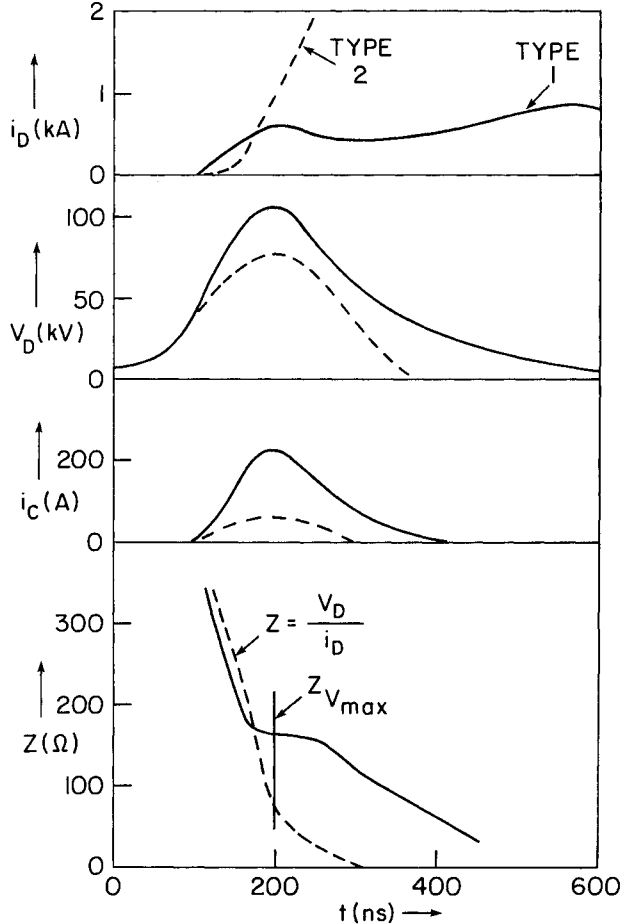


Figure 5. Currents, i_D , voltages, V_D , for the second pulse across the diode. Also shown are the collector currents, i_C , and diode impedances, Z .

Type 2 discharges, indicated by the dashed lines (Fig. 5), result when the delay between pulses is $\leq 100 \mu\text{sec}$ and are not always reproducible. That is, infrequently, type 1 discharges occur at the shorter inter-pulse delay. Note that even though the gap appears to be shorted for type 2 discharges a low current beam may still be produced ($i_C \neq 0$ for type 2 discharges in Fig. 5).

The diode impedance at maximum voltage (V_{max}/I) for various inter-pulse separation times, Δt , is plotted in Figure 6. The triangles are data obtained for type 2 discharges (Fig. 5) and the filled circles are associated with type 1 discharges. The diode impedance is $\sim 300 \Omega$ for $\Delta t \geq 100 \mu\text{sec}$. This agrees with the impedance observed for the first pulse (Fig. 4), i.e., fully recovered diode. Note, however, that even though the impedance is the same for the two pulses, the detailed beam current and voltage waveforms are not identical.

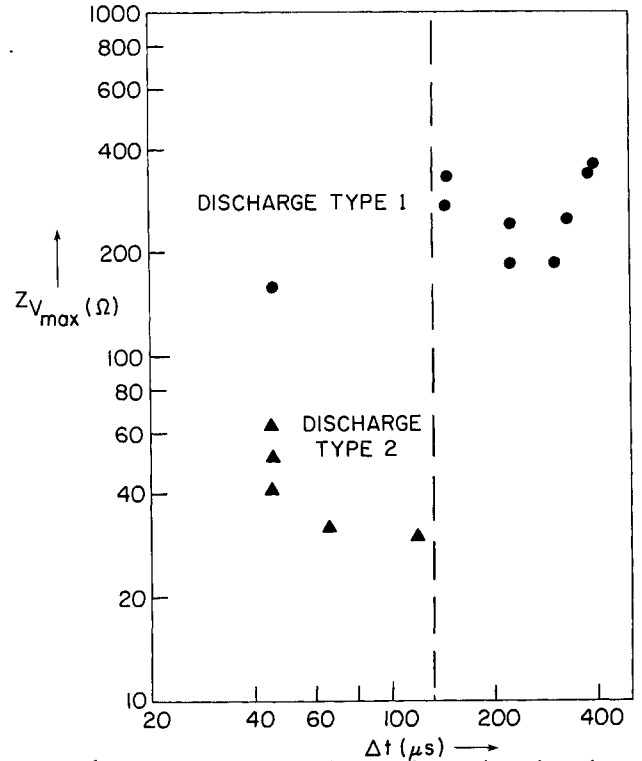


Figure 6. Second pulse diode impedance (at the time of peak voltage) shown as function of the pulse separation time.

V. Discussion

Plasma formation in electron beam diodes using field emission cathodes has been extensively studied. This plasma is associated with explosion of whiskers on the cathode surface which follows stable field emission. These whiskers can carry current densities ranging from 10^6 to 10^8 A/cm^2 , which cause strong local heating. The electric field, F_w , at the whisker tip is enhanced on the order of 100 times, relative to the average applied field across the anode-cathode gap, causing emission of electrons. The electron current is determined by the Child-Langmuir space charge limitation which is modified by the expanding cathode whisker plasma. The effect of the plasma on the diode impedance is determined from both the time of onset of plasma formation, $t_0 = (\rho C / \eta) T_0 F_w$ (where η is the whisker resistivity, C is its heat capacity, ρ is the density and T_0 is the vaporization temperature) and the plasma expansion velocity. The range of t_0 is from 10 to 100 nsec. The typical expansion velocity is 2-4 cm/ μsec , associated with a temperature of few eV. Its density is 10^{17} to 10^{19} cm^{-3} for high current diodes and 10^{15} cm^{-3} for low current diodes. Plasma can also be formed at the anode by virtue of the electron beam depositing its energy in the anode and heating it.¹⁵

Another mechanism for plasma production, which has not been investigated in connection with single-pulse diode studies, is that of plasma formation at both electrodes due to a current flow after the diode impedance has collapsed to very low values. This plasma formation mechanism is that of a vacuum arc,¹³ that is driven by the current remaining in the storage system, and is a typical characteristic of inductively driven systems. It is convenient to consider the two

**R. Parker provides a review of plasma formation mechanisms and their effects on the impedance of high current diodes. The mechanisms outlined here are based on this review.¹⁰

types of plasma, the whisker plasma, generated as a result of very high electric fields, and the arc plasma that arises from the post-pulse current flow and provides a long-time short circuit across the diode. The latter plasma is an especially important factor in diodes driven by the inductive storage pulse, since such systems tend to have an inductive decay time which is longer than the impedance collapse time associated with the whisker plasma expansion.

The results obtained here indicate that indeed a whisker plasma is formed and closes the gap at an average speed of $3\text{--}5 \times 10^6$ cm/sec, as determined by noting the anode-cathode separation and the time, t_p (defined in Fig. 4), at which the diode current is being carried primarily by arc plasma in the diode. This current is supported by the remaining current in the storage system. The arc plasma is observed by the photomultiplier to disappear rapidly (≤ 10 μ sec) when the current flow is stopped by opening fuse wire $FD_{1,2}$, (Fig. 1).

Two mechanisms by which the plasma density in the diode can decrease after the diode current is stopped are plasma expansion (perpendicular to the diode axis) and recombination. The effect of plasma expansion can be estimated assuming that the plasma ceases to affect the diode impedance when

$$n_p \leq n_{CL} = J_{CL}/e\beta c, \quad (1)$$

where n_p is the plasma density, J_{CL} is the Child-Langmuir electron current, n_{CL} is the electron density associated with J_{CL} , c the velocity of light, e the charge on an electron, and βc is the beam velocity ($\beta = [1 - (1 + eV_D/E)^{-2}]^{1/2}$, where E = the electron rest energy). Note that data from the Gamble II generator*** supports this assumption. We further assume that the total number of plasma particles is constant (i.e., neglect recombination) and that n_p is spatially uniform and decreases in time as

$$n(t) = n_0 \frac{r_0^2}{r(t)^2}, \quad (2)$$

where n_0 is the initial plasma density, r_0 is the initial plasma radius, and $r(t) = r_0 + v_r t$ is the plasma radius at time t resulting from radial expansion at speed v_r . Equating n_{CL} from Eq. (1) with the plasma density from Eq. (2) gives the time τ_{CL} ,

$$\tau_{CL} = \frac{r_0}{v_r} \left[\left(\frac{n_0}{n_{CL}} \right)^{1/2} - 1 \right]. \quad (3)$$

For times $\geq \tau_{CL}$ the plasma density should cease to influence the diode behavior. For $V_D = 150$ kV, then $\beta = .63$, and J_{CL} will be 60 A/cm² for a diode separation of 1.5 cm. Assuming $n_0 \approx 10^{16}$ cm⁻³, $r_0 = 1.5$ cm (the diode radius) and further assuming v_r is the same as the axial closing velocity $\approx 4 \times 10^6$ cm/sec (as determined in the preceding paragraph), then τ_{CL} is ≥ 100 μ sec.

An estimate of the recombination (three body and radiative) time¹⁷, τ_R , for various carbon and iron plasmas, assuming the density is constant in time gives $\tau_R \geq 100$ μ sec. This estimate is more sensitive to the density ($\sim n_p$) than the estimate for τ_{CL} . Nevertheless, the two time scales are comparable, $\tau_R \approx \tau_{CL}$, and are close to the observed time for recovery to type 1 operation of Fig. 6.

***Description of the Gamble II generator can be found in Ref. 16

VI. Conclusion

It has been demonstrated that moderate, ~ 150 keV, energy electron beams of ≤ 1 kA current and pulse duration of ~ 500 nsec can be produced from a low voltage, ≤ 10 kV, inductive storage system. Furthermore, the system can be double pulsed with a variable interpulse separation time of 10-500 μ sec.

The diode can recover in times ≥ 100 μ sec. The recovery is not total, even with a 500 μ sec inter-pulse separation time, in that the detailed time histories of the beam current and voltage are not identical for the two pulses. This is most likely due to the presence in the diode of a low level of plasma and neutrals associated with the first pulse; although, the second pulse circuitry may also contribute to some of the differences. The choice of parameters in the work described here is reasonable for scaling these results to diodes operating in the megavolt and tens of kiloamperes regime.

Work supported by the Office of Naval Research.

^aJAYCOR, Inc., 205 S. Whiting St., Alexandria, VA 22302

^bInstitut Fuer Hochspannungs Technik, Braunschweig, Federal Republic of Germany

References

1. M. T. Buttram, 2nd International Pulsed Power Conf., Lubbock, Texas (1979).
2. G. Yonas, A. J. Toepfer in "Gaseous Electronics," Vol. 1, M. M. Hirsch and H. J. Oskam, eds., (Academic Press, 1978), Ch. 6.
3. Yu. A. Kotov, B. M. Kovalchuk, N. G. Kolganov, G. A. Mesyats, V. S. Sedoi, A. L. Ipatov, Sov. Tech. Phys. Lett. **3**(9), 359 (1977).
4. B. M. Kovalchuk, Yu. A. Kotov, G. A. Mesyats; Sov. Phys. Tech. Phys. **19**(1), 136 (1974).
5. J. Salge, U. Braunsberger, U. Schwarz; 1st Int. Conf. Energy, Compression and Switching, Torino, (1974).
6. I. M. Vitkovitsky, D. Conte, R. D. Ford, W. H. Lupton, NRL Memorandum Report 4168 (1980).
7. R. D. Ford, I. M. Vitkovitsky, IEEE Trans. on Electron Devices **ED-26**, 1527 (1979).
8. L. V. Dubovoi, I. M. Roife, E. V. Seredenko, B. A. Stekolnidov, Efremov Institute Report No. OT-5, Leningrad, USSR, (1974).
9. M. Friedman, M. Ury, Rev. Sci. Instr. **41**, 1334 (1970).
10. R. K. Parker, R. E. Anderson, C. V. Duncan, J. App. Phys. **45**, 2463 (1974).
11. R. A. Gilmour, R. F. Hope, R. N. Miller, IEEE 14th Pulse Power Modulator Symposium, (1980).
12. I. M. Vitkovitsky, V. E. Scherrer, to be published in J. App. Phys.
13. T. H. Lee "Physics and Engineering of High Power Switching Devices," (MIT press, 1975), Ch. 5,6.
14. E. J. Henley, D. Richman, Analytical Chem. **28**, 1580 (1956).
15. A. E. Blaugrund, G. Cooperstein, Physics of Fluids, **20**, 1158 (1977).
16. L. S. Levine, I. M. Vitkovitsky, IEEE Tran. Nuc. Sci. **NS-18**, 255 (1971).
17. R. C. Elton, "Methods of Experimental Physics," Vol. A, Griem and Lovberg, eds., (Academic Press, 1970) Ch. 4.